Appl. Phys. A 49, 95–103 (1989)

Applied Physics A Solids and Surfaces

Non-Faradaic Electrochemical Modification of Catalytic Activity in Solid Electrolyte Cells

C. G. Vayenas*, S. Bebelis, S. Neophytides, and I. V. Yentekakis

Institute of Chemical Engineering and High Temperature Chemical Processes, Department of Chemical Engineering, University of Patras, Patras 26110, Greece

Received 25 October 1988/Accepted 9 March 1989

Abstract. The catalytic activity and selectivity of metal catalysts used as electrodes in high temperature solid electrolyte cells can be altered dramatically and in a reversible manner. This is accomplished by electrochemically supplying oxygen anions onto catalytic surfaces via polarized metal-solid electrolyte interfaces. Oxygen anions, forced electrochemically to adsorb on the metal catalyst surface, alter the catalyst work function in a predictable way and lead to reaction rate increases as high as 4000%. Changes in catalytic rates typically exceed the rate of O^{2-} transport to or from the catalyst surface by 10^2–$3 \cdot 10^5$. Significant changes in product selectivity have been also observed. The case of several catalytic reactions in which this new phenomenon has been observed is presented and the origin of the phenomenon is discussed.

PACS: 85.80, 82.20, 82.65, 73.20

Since the pioneering work of Kiukkola and Wagner [1], solid-state electrochemical cells involving oxygen-ion-conducting solid electrolytes have been investigated extensively for fuel cell applications [2–8], for steam electrolysis [9, 10] and for chemical cogeneration, i.e., for the simultaneous generation of chemicals and electric power in solid electrolyte fuel cell reactors [11–18]. However, so far the only commercial use of solid electrolyte cells has been as oxygen sensors, particularly for monitoring and control of combustion processes [19, 20].

The interesting role that solid electrolyte cells can play in the study of heterogeneous catalysis was first realized by Wagner [21] who proposed the use of such cells for the measurement of the activity of oxygen on metal catalysts. The experimental feasibility of this in situ technique, which is usually called solid electrolyte potentiometry (SEP) has been demonstrated in a number of studies since 1979 [22–26] where kinetic and simultaneous SEP measurements were combined to investigate the mechanism of several catalytic oxidations on metals. The SEP technique is particularly suitable for the study of oscillatory reactions [25, 26].

More recently, a far more interesting and somehow surprising application of solid electrolyte cells in the area of heterogeneous catalysis has been discovered. It has been known for some years that solid electrolyte cells operating in the oxygen "pump" mode can be used to promote electrocatalytically the rate of several reactions such as NO decomposition [27, 28], CO hydrogenation [29, 30], methane conversion to C_2 hydrocarbons [31, 32] and propylene conversion to acrolein [33]. In two such studies involving ethylene and propylene epoxidation on Ag electrodes [34–36] it was observed that the behaviour was non-Faradaic in the sense that the increase in the rates of olefin epoxidation and conversion to CO_2 would typically exceed the rate of O^{2-} transport to or from the electrolyte by a factor of 300, suggesting dramatic and reversible changes in the catalytic properties of the catalyst-electrode.

Very recently this new phenomenon of non-Faradaic electrochemical modification of catalytic activity (NEMCA) has been studied systematically for the reactions of CO oxidation on Pt [37], ethylene

* To whom correspondence should be addressed

oxidation on Pt [38, 39] and methanol dehydrogenation and decomposition on Ag [38, 40]. Dramatic changes in catalytic activity and selectivity were observed with all these reactions. It was found that catalyst activity usually depends exponentially on catalyst potential and it was proposed that the NEMCA effect is due to changes in catalyst work function caused by the interaction of the catalyst surface with excess O^{2-} pumped electrochemically through the solid electrolyte.

In this work we identify the common features of previous studies of the NEMCA effect, [37–40], report new results for the reactions of CH_3OH, C_2H_4, and CO oxidation on Pt, CO oxidation on Pd and C_2H_4 partial oxidation on Ag and discuss the origin of the effect in terms of the influence of changing catalyst work function on the strength of chemisorptive bonds and on catalytic activity.

1. Experimental

The experiments have been carried out in solid electrolyte cells of the type:

gaseous reactants, metal catalyst

$$|ZrO_2\ (8\ mol\%\ Y_2O_3)|M, O_2, \quad (1)$$

where the metal M catalyzes the reaction

$$(1/2)O_2 + 2e^- \rightleftharpoons O^{2-} \quad (2)$$

and serves as a means of supplying O^{2-} to the catalyst through the yttria-stabilized-zirconia electrolyte under the influence of an external voltage. The zirconia reactor-cell shown in Fig. 1 has been described in detail elsewhere [26, 37–40]. Figure 2 shows the electrode configuration on the zirconia tube bottom. This three-electrode system used on conjunction with the current

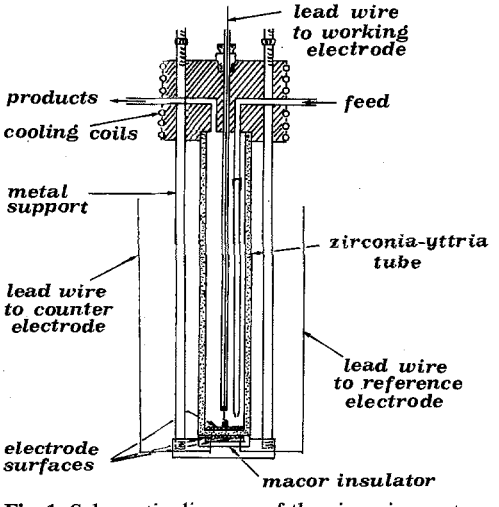

Fig. 1. Schematic diagram of the zirconia reactor

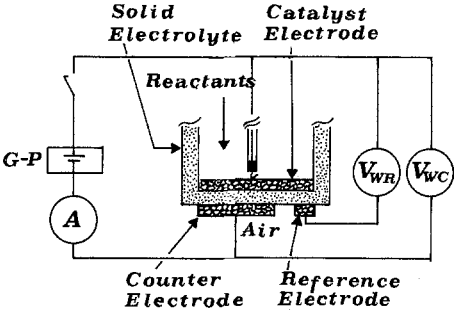

Fig. 2. Electrode configuration; G-P: Galvanostat-Potentiostat

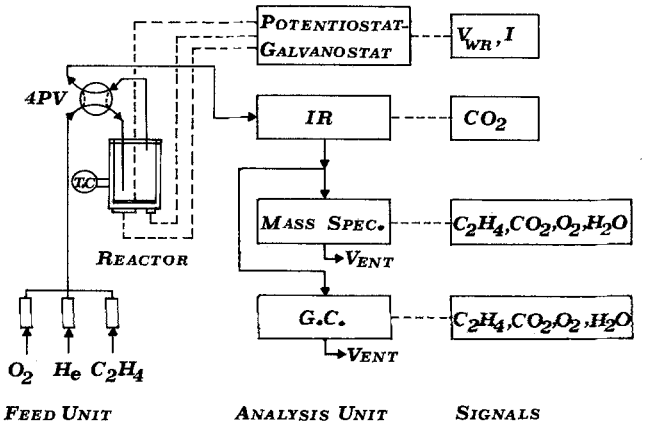

Fig. 3. Schematic diagram of the apparatus. Reactants and products refer to the case of C_2H_4 oxidation on Pt

interruption technique and utilizing a Hameg memory oscilloscope permits accurate measurement of the catalyst-electrode overpotential η and of the catalyst-solid electrolyte exchange current density i_0, as described in detail elsewhere [37–39]. The experimental apparatus shown schematically in Fig. 3 and described in detail elsewhere [26, 37–40] utilizes on-line gas-chromatography (Perkin-Elmer Sigma 300), mass spectrometry (Balzers QMG 311) and IR spectroscopy (Beckman 864) for continuous analysis of the zirconia reactor feed and products.

Porous Pt, Pd, and Ag catalyst and auxiliary electrode films are deposited on the stabilized zirconia electrolyte using Pt and Pd Engelhard pastes and Ag solutions in butyl acetate followed by calcination at temperatures on the order of 1000 K as described in detail in previous studies [23, 26, 34–40] where catalyst characterization details are also presented. The porous catalyst films have typically thicknesses on the order of 5 μm, porosities on the order of 30%, superficial surface areas of 2 cm^2 and true surface areas on the order of 200 cm^2 as measured by surface titration techniques using O_2 and CO [23, 26, 34, 36].

During the experiments both the galvanostatic and potentiostatic mode of operation have been tested,

using an AMEL 553 galvanostat-potentiostat. Both modes have been found to give qualitatively the same results. In the galvanostatic mode a constant current I is applied between the catalyst (working electrode) and the counter electrode and the catalyst potential is monitored vs the reference electrode, which is in contact with air. In the potentiostatic mode a constant potential is applied between the catalyst and the reference electrode and the current is monitored between the catalyst and the counter electrode. All results reported here have been obtained galvanostatically.

As in previous papers [34–40] we have defined the current I to be positive when O^{2-} are pumped *to* the catalyst and negative when O^{2-} are removed *from* the catalyst.

2. Results

2.1. Definitions

Table 1 lists the catalytic reactions which have been shown so far to exhibit the NEMCA effect. For the reactions marked with an asterisk kinetic measurements have been obtained with simultaneous accurate measurements of the catalyst-solid electrolyte activation overpotential η. We have found no catalytic reaction yet which does not exhibit the NEMCA effect in the presence of significant (i.e. a few hundred mV) activation overpotential η. In order to compare different reactions it is useful to define two quantities, i.e. the enhancement factor Λ [18, 37–40] and the rate enhancement ratio ϱ. The former quantity is defined from

$$\Lambda = \Delta r(\text{catalytic})/(I/2F), \tag{3a}$$

Table 1. List of catalytic reactions found to exhibit the NEMCA effect

	Reactants	Products	Catalyst	T [°C]	Λ range	ϱ range	Ref.
1	$CH_2=CH_2$, O_2	ethylene oxide, CO_2	Ag	320–420	[0, +300]	< 3	34, 35, this work[a,b]
2	propylene, O_2	propylene oxide, CO_2	Ag	320–420	[0, +300]	< 2	36[a]
3	$CH_2=CH_2$, O_2	CO_2	Pt	260–420	$[0, +3\cdot10^5]$	<55	39[b], this work[b]
4	CO, O_2	CO_2	Pt	300–550	[−500, +500]	< 6	37, this work[b]
5	CO, O_2	CO_2	Pd	550–400		< 1.5	this work[b]
6	CH_3OH, O_2	CO_2, H_2CO	Pt	300–500	$[-3\cdot10^4, +10^4]$	<10	this work[a,b]
7	CH_3OH	H_2CO, CO, CH_4	Pt	400–500	[−10, 0]	< 3	42[a,b]
8	CH_3OH	H_2CO, CO, CH_4	Ag	550–750	[−25, 0]	< 6	40[a,b]

[a] Change in product selectivity observed

[b] η, V_{WR} measured within ±5 mV using a three-electrode system in conjunction with the current-interruption technique and an oscilloscope

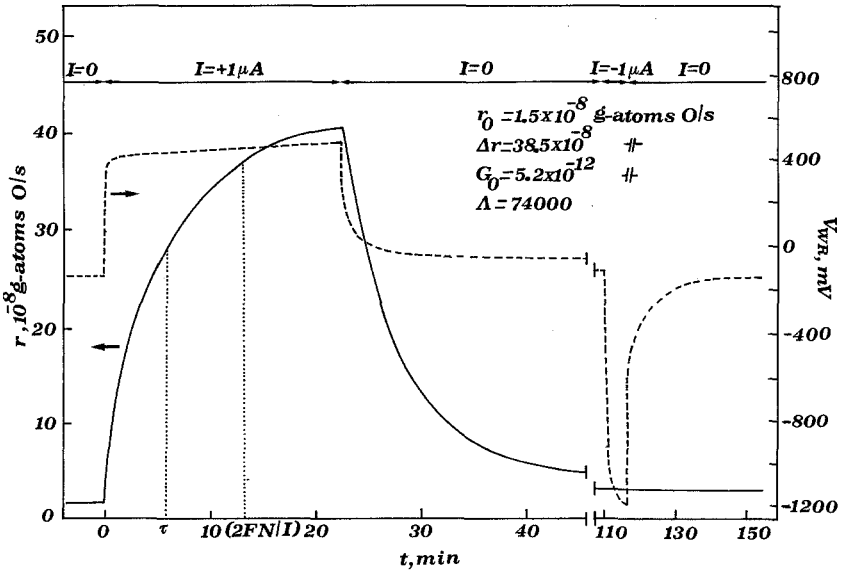

Fig. 4. Typical catalytic rate response to step changes in cell current (galvanostatic transients); comparison of experimental (τ) and computed ($2FN/I$) relaxation time constants; C_2H_4 oxidation on Pt; $T=370$°C, $p_{O_2}=4.6\cdot10^{-2}$ bar, $P_{ET}=3.6\cdot10^{-3}$ bar, $N=4.2\cdot10^{-9}$ g-atoms

where $I/2F$ is the rate of O^{2-} transport to or from the catalyst, which at steady state equals the net rate of the electrocatalytic reaction (2). A reaction exhibits the NEMCA effect when $|\Lambda| \gg 1$. As shown in Table 1, $|\Lambda|$ values on the order of 10^4–$3 \cdot 10^5$ have been measured for some reactions.

The rate enhancement ratio ϱ is defined by

$$\varrho = r(\text{catalytic})/r_0(\text{catalytic}), \tag{3b}$$

where r_0 denotes the regular catalytic, i.e., open-circuit catalytic rate. As shown in Table 1, ϱ values of order 5–50 have been obtained with several catalytic reactions. An example is shown in Fig. 4 for the case of C_2H_4 oxidation on Pt.

A third important parameter in describing the NEMCA effect is the rate increase relaxation constant τ observed during a galvanostatic transient. This is defined as the time required for the catalytic rate increase to reach 63% of its final steady-state value during a galvanostatic transient. Typical measured τ values are on the order of 10^2–10^4 s as also shown in Fig. 4.

2.2 *Common Features of the NEMCA Effect in Different Catalysts and Reactions*

Despite the differences in open-circuit catalytic behaviour of the reactions shown in Table 1 and despite the dramatic differences in the observed enhancement factors Λ, there are three important similarities which can be summarized as follows:

i) Over wide ranges of overpotential η or catalyst potential relative to the reference electrode V_{WR}, the catalytic rates r or kinetic constants K depend exponentially on catalyst potential, i.e.

$$\ln(r/r_0) = \alpha F(V_{WR} - V^*_{WR})/RT, \tag{4}$$

where α and V^*_{WR} are catalyst- and reaction-specific constants. Examples are shown in Fig. 5 for the cases of C_2H_4 and CH_3OH oxidation on Pt. Consequently the rate enhancement ratio $\varrho = r/r_0$ is basically determined by the catalyst potential V_{WR}, or, equivalently by the catalyst-solid electrolyte overpotential

$$\eta (= V_{WR} - V^o_{WR}),$$

and not by the current.

ii) The observed enhancement factors Λ are on the order of $2Fr_0/I^o$, where I^o is the current at a potential equal to V^*_{WR} [39, 40]. The parameter I^o is proportional to the catalyst-solid electrolyte exchange current I_0, therefore Λ is proportional to the intrinsic catalytic rate r_0 and inversely proportional to the catalyst-solid electrolyte exchange current I_0 [38–40]. Consequently, in order to obtain a strong NEMCA effect, i.e., high Λ values for a given catalytic reaction, one must use a highly polarizable, i.e., low I_0, catalyst-solid electrolyte interface.

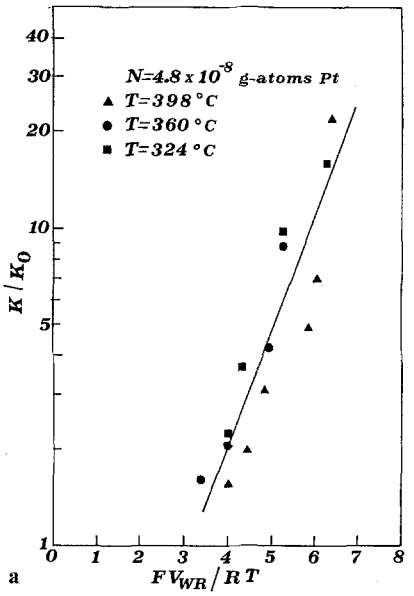

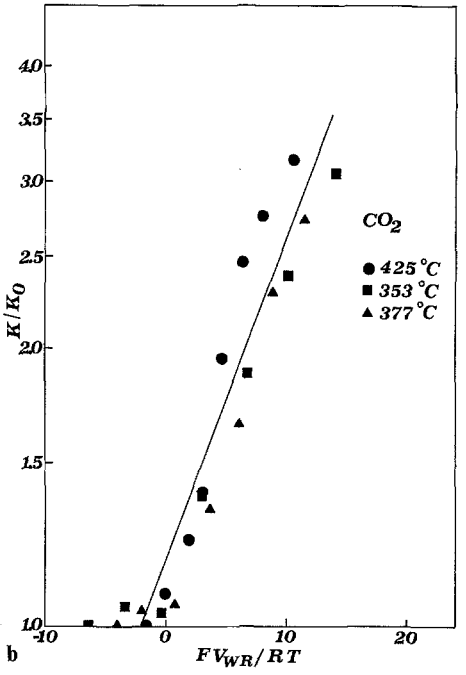

Fig. 5a, b. Effect of catalyst potential V_{WR} and of the dimensionless parameter $\Pi = FV_{WR}/RT$ on the kinetic constants of catalytic reactions: **a** C_2H_4 oxidation on Pt, **b** CH_3OH oxidation to CO_2 on Pt

iii) The rate increase relaxation time constants τ are on the order of $2FN/I$, where N is the number of surface catalyst g-atoms. The measurement of N, which is, of course, proportional to the catalyst surface area, using surface titration techniques, has been described in detail elsewhere [23, 26, 34, 36]. This observation shows that the catalytic properties of the

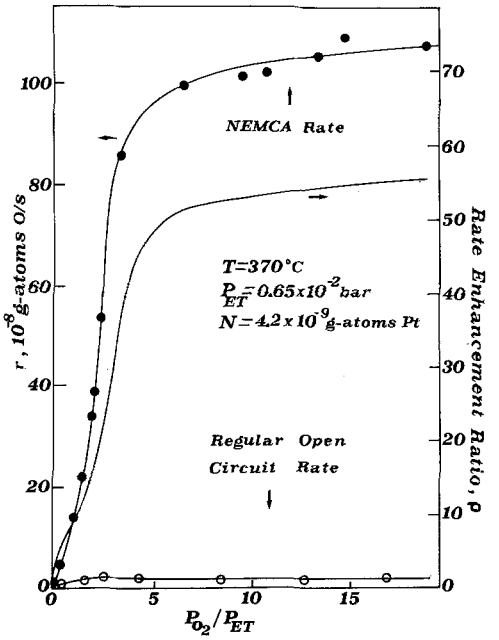

Fig. 6. Effect of gaseous composition on regular (open-circuit) and NEMCA induced reaction rate ($V_{WR}=1$ V) and on the rate enhancement ratio ϱ for a preoxidized Pt catalyst during C_2H_4 oxidation to CO_2; $N=4.2\cdot10^{-9}$ g-atoms

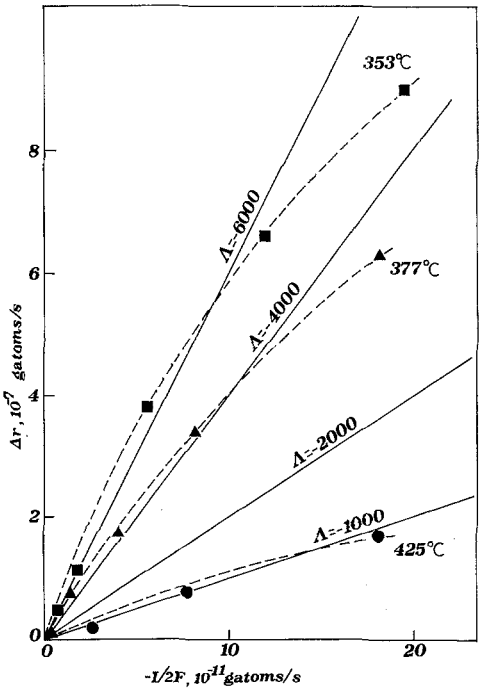

Fig. 7. Effect of the rate of O^{2-} removal ($I/2F$) from a Pt catalyst during CH_3OH oxidation to H_2CO and CO_2 on the total rate of atomic oxygen consumption on the catalyst; $p_{CH_3OH}=8\cdot10^{-3}$ bar, $p_{O_2}=0.18$ bar, solid lines are constant enhancement factor lines

entire catalyst surface change during electrochemical oxygen pumping, probably due to the surface diffusion (spillover) of oxygen anions, most probably O^- [38–40]. This is strongly supported by recent investigation of Ag electrodes in zirconia cells using in situ XPS which showed the appearance of an O 1*s* signal corresponding to ionically bonded oxygen during electrochemical oxygen pumping [41].

2.3. Ethylene Oxidation on Pt

The kinetics of this reaction have been described in detail recently [39]. Figure 6 shows the effect of the oxygen to ethylene ratio on the regular catalytic (open-circuit) rate and on the NEMCA induced rate of CO_2 formation at a constant catalyst potential $V_{WR}=1$ V. The rate enhancement ratio $\varrho=r/r_0$ is on the order of 55 for high oxygen to ethylene ratios. Figure 5a was obtained with a different catalyst film under fuel-lean conditions, i.e., $p_{O_2}\gg P_{ET}$, where the rate is first order in ethylene, i.e., $r=KP_{ET}$ [25, 39]. As shown on this figure the kinetic constant K depends exponentially on V_{WR}. This is an example of the generally observed kinetic behaviour described by (4). Enhancement factors Λ as high as $3\cdot10^5$ have been observed for this reaction [39].

2.4. Methanol Oxidation on Pt

The open-circuit kinetic behaviour of this system has been studied in detail recently [42]. The main products are H_2CO and CO_2. This reaction is particularly interesting because it exhibits both the positive ($I>0$, $\Lambda>0$) and negative ($I<0$, $\Lambda<0$) NEMCA effect, as shown in Fig. 5b for positive currents and in Figs. 7 and 8 for negative currents.

Figure 7 shows the effect of O^{2-} removal from the catalyst, i.e. $I/2F$, on the increase in the total rate of O consumption on the catalyst surface, due to the reactions:

$$CH_3OH + (1/2)O_2 \rightarrow H_2CO + H_2O, \quad (5)$$

$$CH_3OH + (3/2)O_2 \rightarrow CO_2 + 2H_2O. \quad (6)$$

The solid lines on Fig. 7 are lines of constant enhancement factor Λ. As shown in Fig. 8 the (2nd order [42]) kinetic constants of H_2CO and CO_2 formation, depend exponentially on the dimensionless parameter $\Pi=FV_{WR}/RT$. This again conforms to the general observation described by (4), with negative α values. Product selectivity also changes significantly with V_{WR} and Π, as can be easily seen by comparing Figs. 8a and b.

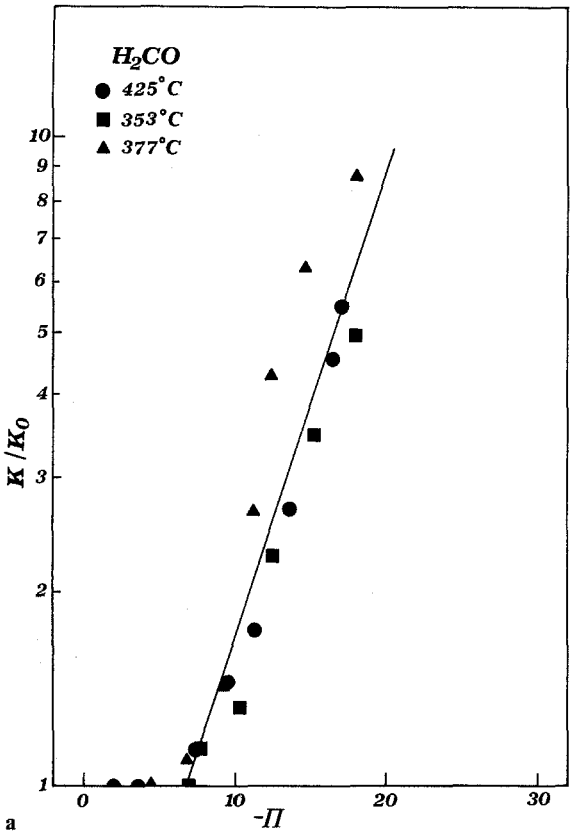

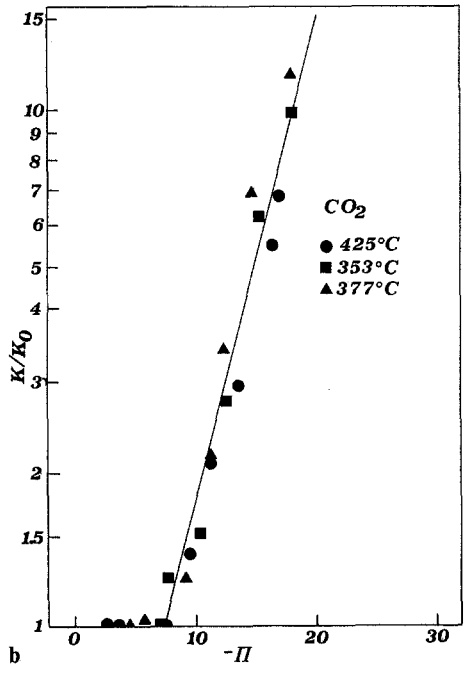

Fig. 8a, b. Effect on $\Pi = FV_{WR}/RT$ on the kinetic constants of CH_3OH oxidation to H_2CO **a** and CO_2 **b** on Pt upon O^{2-} removal from the catalyst

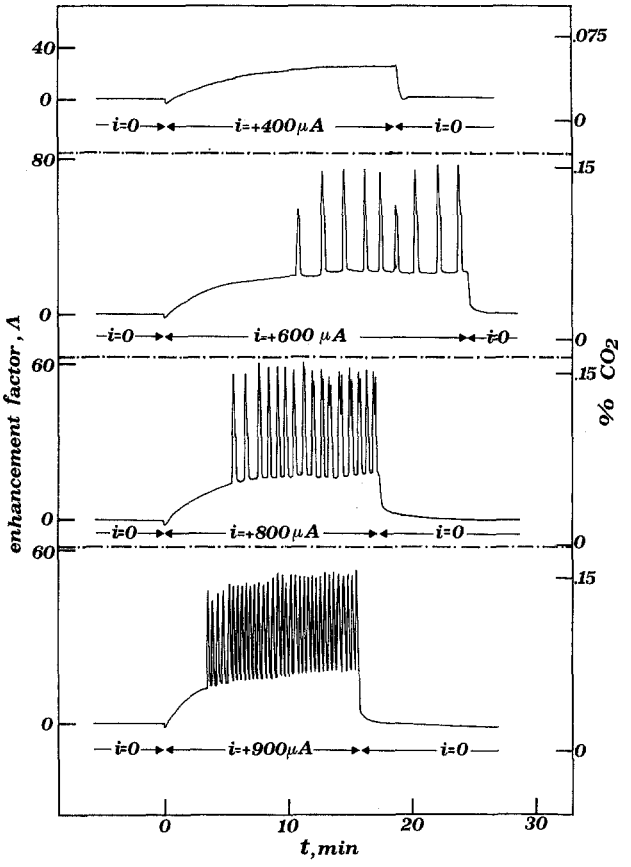

Fig. 9. NEMCA induced rate increase and kinetic oscillations during CO oxidation on Pt; total molar flow rate $1.85 \cdot 10^{-4}$ mole/s; $T = 355$°C; inlet conditions: $p_{CO} = 1.1 \cdot 10^{-2}$ bar, $p_{O_2} = 0.17$ bar

2.5. *CO Oxidation on Pt and Pd*

These are well known oscillatory reactions [25, 44] and both were found to exhibit the NEMCA effect. In the case of the Pd catalyzed CO oxidation Λ values on the order of 10^3 were measured at $T = 290$°C, $p_{CO} = 3.10^{-4}$ bar, and $p_{O_2} = 0.15$ bar. The Pt catalyzed CO oxidation has already been shown to exhibit a strong NEMCA effect [37]. Figure 9 shows the induction of oscillatory states by the NEMCA effect, i.e., by application of small positive currents to a Pt catalyst which is in a non-oscillatory steady state under open-circuit, i.e. regular catalytic conditions.

2.6. *Ethylene Epoxidation on Ag*

This was the first reaction for which a non-Faradaic behaviour was observed upon O^{2-} pumping, without however utilizing a three-electrode system to measure η and V_{WR} [34, 35]. In this work η and V_{WR} have been measured accurately and typical results are shown in Fig. 10 for the rates of ethylene oxide and CO_2 formation. As shown on the figure, changing V_{WR}

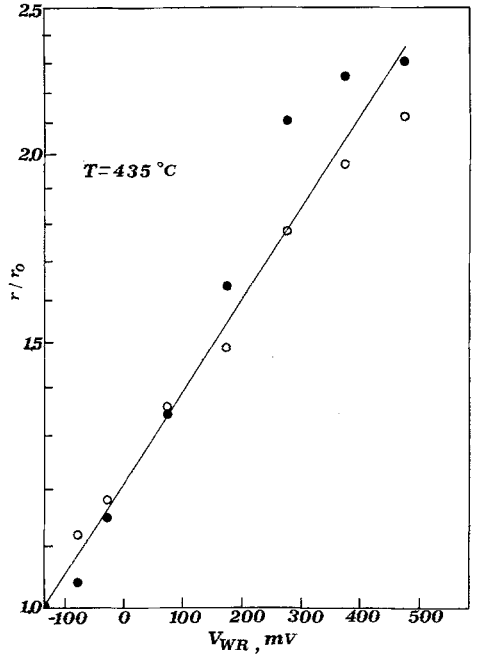

Fig. 10. Effect of Ag catalyst potential V_{WR} on the rates of ethylene epoxidation (open symbols) and ethylene oxidation to CO_2 (filled symbols); total molar flow rate $4.1 \cdot 10^{-5}$ mole/s; $T=435$°C; $p_{C_2H_4}=2.49 \cdot 10^{-2}$ bar, $p_{O_2}=3.45 \cdot 10^{-2}$ bar

affects exponentially both reactions rates. Detailed results for this reaction system, for which product selectivity is also significantly affected under certain conditions, will appear elsewhere [44].

3. Discussion

The catalytic reactions which have been found so far to exhibit the NEMCA effect in stabilized zirconia cells are shown in Table 1. Since no reaction has been found yet for which a NEMCA effect is not obtained in the presence of significant (i.e. a few hundred mV) catalyst-solid electrolyte overpotential, it appears that the NEMCA effect may be of general interest in the field of heterogeneous catalysis. Consequently the controlled modification of catalytic activity and selectivity may become an important application of solid electrolytes.

In order to explain the experimental observation

$$\ln(r/r_0)=\alpha F(V_{WR}-V_{WR}^*)/RT \tag{4}$$

which has been found to describe the observed kinetic behaviour over wide ranges of catalyst potential V_{WR} both for the present work and for all other systems where the effect of O^{2-} pumping has been studied with simultaneous accurate measurement of the overpotential η and of the catalyst potential V_{WR}, one must first examine the effect of O^{2-} pumping and of the appearance of activation overpotential η on the electronic properties of the metal catalyst. This question has been addressed in detail in two recent communications describing the NEMCA effect during C_2H_4 oxidation on Pt [39] and CH_3OH dehydrogenation and decomposition on Ag [40]. Using the standard definitions of inner (or Galvani) potential, outer (or Volta) potential Ψ, electrochemical potential of electrons (or Fermi level) $\bar{\mu}_e$ and work function $e\Phi$ [45], it was shown that the catalyst potential with respect to the reference electrode, i.e., V_{WR} is given by

$$V_{WR}=(\Phi_W-\Phi_R)+(\Psi_W-\Psi_R), \tag{7}$$

where the subscripts W and R refer to the working electrode (catalyst) and to the reference electrode respectively. The Ψ, or Volta, potentials are nonzero only when there is a net charge on the metal surface. Equation (7) is valid both under open-circuit and closed-circuit conditions. For open-circuit (i.e. SEP) measurements it implies that the open-circuit emf V_{WR}^o provides a measure of the catalyst work function in relation to the reference electrode work function, provided that no net charge develops on the two-electrodes, i.e., $\Psi_W=\Psi_R=0$.

When the circuit is closed, i.e., during O^{2-} pumping, the reference electrode remains unaffected, i.e. Φ_R and Ψ_R remain constant. Consequently (7) can be written as

$$\eta=V_{WR}-V_{WR}^o=(\Phi_{W(I)}-\Phi_{W(I=0)}) +(\Psi_{W(I)}-\Psi_{W(I=0)}). \tag{8}$$

Equation (8) has been derived rigorously and without making any assumptions. In order to further exploit this equation one must examine the magnitude of the last term $\Psi_{W(I)}-\Psi_{W(I=0)}$ on the catalyst surface exposed to the gas phase. First it is worth noting that $\bar{\mu}_{e,W}$ is the same throughout the bulk of the catalyst. However Φ_W and Ψ_W, the sum of which equals $-\bar{\mu}_e/e$ [45], need not be the same over the entire catalyst surface if the catalyst-electrode carries a net charge which is not uniformly distributed on the catalyst surface. Such a net charge may exist but will be localized at the metal-solid electrolyte interface, which is usually modelled as a resistor and a capacitor connected in parallel. However what is of interest here are changes in Φ_W and Ψ_W on the metal-electrode surface which is catalytically active, i.e., which is exposed to the gas phase and which in our porous films has a surface area 2 to 4 orders of magnitude higher than the surface area of the metal-solid electrolyte interface. Any ions or molecules directly adsorbing on the catalytically active surface will be paired with a compensating charge in the metal. The effect of such ion-electron pairs produced by adsorption from the gas phase would be included in a work function

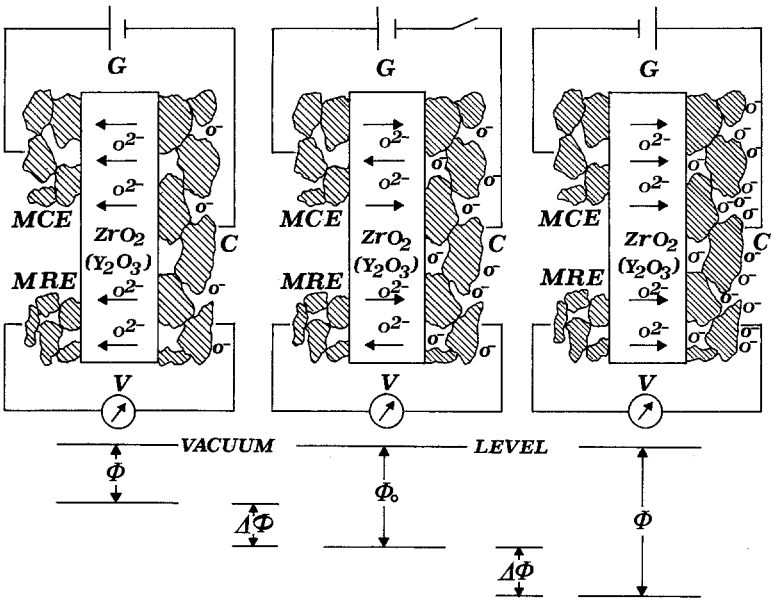

Fig. 11. Schematic representation of the origin of NEMCA. Effect of negative and positive currents on the relative concentrations of oxygen anions on the catalyst Fermi level $E_F = \bar{\mu}_e$ and in work function $e\Phi$ of the catalyst surface; C: Catalyst, MCE: Metal counter electrode, MRC: Metal reference electrode

measurement and therefore must be included within Φ_W and not Ψ_W. Consequently, when the Φ_W and Ψ_W terms in (7) and (8) refer to the catalytically active surface area of the catalyst-electrode, then the Ψ_W terms vanish and one can rewrite these equations as

$$V_{WR} = \Phi_W - \Phi_R, \tag{9}$$

$$\eta = V_{WR} - V^o_{WR} = \Phi_{W(I)} - \Phi_{W(I=0)}. \tag{10}$$

Equation (10) implies that when $\eta > 0$, i.e. $V_{WR} > V^o_{WR}$, or equivalently when O^{2-} ions are pumped to the catalyst surface, then there is an increase in the catalyst work function $e\Phi_W$ equal to $e\eta$. The opposite happens when $V_{WR} < V^o_{WR}$, i.e., there is a decrease in the average catalyst surface work function. The situation is depicted schematically in Fig. 11, where no attempt was made to show the compensating charges in the metal.

When the catalyst work function changes, the Fermi level of electrons in the catalyst changes and therefore there is an increase ($e\Delta\Phi_W < 0$) or decrease ($e\Delta\Phi_W > 0$) in the availability of electrons for chemisorptive bond formation. This leads to stronger or weaker bonding, respectively, between the catalyst and all chemisorbed species with a concomitant increase or decrease, respectively, in the heats of chemisorption ($-\Delta H_{ad}$). According to early theoretical considerations of Boudart [46] it should be

$$\Delta(-\Delta H_{ad}) = -(n/2)e\Delta\Phi \tag{11}$$

where n is the number of valence electrons of the adatom taking part in the bonding. Despite its simplicity, (11) has been found on several occasions to be in good agreement with experiment [46]. On the basis of (10) and (11) one can then explain the observed exponential dependence of the rates on η and V_{WR} (4) by noting that η and $\Delta\Phi$ are linearly related to the changes in catalyst work function $e\Delta\Phi$ (10), therefore to the induced changes in the heats of adsorption (11), which are expected from classical activated complex kinetic considerations to induce exponential changes in the catalytic rates [38–40].

In summary solid electrolyte cells with porous metal electrodes can be used to influence the work function of metal catalysts and to induce dramatic changes in catalytic activity and selectivity. Although only the reactions shown in Table 1 have been investigated so far, it is very likely that new technological applications can emerge as more reactions are explored.

Acknowledgements. Financial support from the VW Stiftung of the Federal Republic of Germany and from the European Economic Community Non-nuclear Energy Program is gratefully acknowledged. We also thank Professor L. Riekert for helpful discussions.

References

1. K. Kiukkola, C. Wagner: J. Electrochem. Soc. **104**, 79 (1957)
2. T.H. Etsell, S.N. Flengas: J. Electrochem. Soc. **118**, 1890 (1971)
3. B.C.H. Steele: In *Electrode Processes in Solid State Ionics*, ed. by M. Kleitz, J. Dupuy (Reidel, Dordrecht 1976)
4. E.C. Subbarao: *Solid Electrolytes and their Applications* (Plenum, New York 1980)
5. A.O. Isenberg: Solid State Ionics **3/4**, 431 (1981)
6. E.C. Subbarao, H.S. Maiti: Solid State Ionics **11**, 317 (1984)
7. C.G. Vayenas, P.G. Debenedetti, I.V. Yentekakis, L.L. Hegedus: I & EC Fundamentals **24**, 316 (1985)
8. J.N. Michaels, C.G. Vayenas, L.L. Hegedus: J. Electrochem. Soc. **133**, 522 (1986)

9. E.J.L. Schouler, M. Kleitz, E. Forest, E. Fernandez, P. Fabry: Solid State Ionics **5**, 559 (1981)
10. G.B. Barbi, C.M. Mari: Solid State Ionics **6**, 341 (1982)
11. C.G. Vayenas, R.D. Farr: Science **208**, 593 (1980)
12. R.D. Farr, C.G. Vayenas: J. Electrochem. Soc. **127**, 1478 (1980)
13. C. Sigal, C.G. Vayenas: Solid State Ionics **5**, 567 (1981)
14. J.N. Michaels, C.G. Vayenas: J. Catal. **85**, 477 (1984)
15. J.N. Michaels, C.G. Vayenas: J. Electrochem. Soc. **131**, 2544 (1984)
16. N. Kiratzis, M. Stoukides: J. Electrochem. Soc. **134**, 1925 (1987)
17. I.V. Yentekakis, C.G. Vayenas: J. Electrochem. Soc. **136**, 996 (1989)
18. C.G. Vayenas: Solid State Ionics **28–30**, 1521 (1988)
19. W.L. Worrell: In *Electrochemistry and Solid State Science Education*, ed. by W.R. Smyrl, F. McLarnon (The Electrochemical Society, Pennington, NJ 1986)
20. W. Kernler, B. Leibold, A. Löbert, N. Nicolose, W. Weppner: Proc. 6th Intern. Conf. on Solid State Ionics, ed. by W. Weppner (1988) (North-Holland, Amsterdam 1988)
21. C. Wagner: Adv. Catal. **21**, 373 (1970)
22. C.G. Vayenas, H.M. Saltsburg: J. Catal. **57**, 296 (1979)
23. M. Stoukides, C.G. Vayenas: J. Catal. **82**, 45 (1983)
24. E. Häfele, H.-G. Lintz: Ber. Bunsenges. Physik Chem. **90**, 298 (1986)
25. C.G. Vayenas, B. Lee, J.N. Michaels: J. Catal. **66**, 36 (1980)
26. I.V. Yentekakis, S. Neophytides, C.G. Vayenas: J. Catal. **111**, 152 (1988)
27. S. Pancharatnam, R.A. Huggins, D.M. Mason: J. Electrochem. Soc. **122**, 869 (1975)
28. T.M. Gür, R.A. Huggins: J. Electrochem. Soc. **126**, 1067 (1979)
29. T.M. Gür, R.A. Huggins: Science **219**, 967 (1983)
30. T.M. Gür, G.A. Huggins: J. Catal. **102**, 443 (1986)
31. K. Otsuka, S. Yokoyama, A. Morikawa: Chem. Lett. Chem. Soc. Jpn. 319 (1985)
32. S. Seimanides, S. Stoukides: J. Electrochem. Soc. **133**, 1535 (1986)
33. T. Hayakawa, T. Tsunoda, H. Orita, T. Kameyama, T. Takahashi, K. Takehira, K. Fukuda: J. Chem. Soc. Jpn. Chem. Commun. 961 (1986)
34. M. Stoukides, C.G. Vayenas: J. Catal. **70**, 137 (1981)
35. M. Stoukides, C.G. Vayenas: ACS Symp. Series **178**, 181 (1982)
36. M. Stoukides, C.G. Vayenas: J. Electrochem. Soc. **131**, 839 (1984)
37. I.V. Yentetakis, C.G. Vayenas: J. Catal. **111**, 170 (1988)
38. C.G. Vayenas, S. Bebelis, S. Neophytides: J. Phys. Chem. **92**, 5083 (1988)
39. S. Bebelis, C.G. Vayenas: J. Catal. (1989) (in press)
40. S. Neophytides, C.G. Vayenas: J. Catal. (1989) (in press)
41. T. Arakawa, A. Saito, J. Shiokawa: J. Appl. Surf. Sci. **16**, 365 (1983)
42. S. Neophytides: Ph.D. Thesis, U. of Patras (1988)
43. B.C. Sales, J.E. Turner, M.B. Maple: Surface Science **114**, 381 (1982)
44. S. Bebelis, C.G. Vayenas (in preparation)
45. P.M. Gundry, F.C. Tompkins: In *Experimental Methods in Catalytic Research*, ed. by R.B. Anderson (Academic, New York 1968) pp. 100–168
46. M. Boudart: J. Am. Chem. Soc. **74**, 3556 (1952)